Industrial use of equivalent sand grain height models for roughness modelling in turbomachinery

Emma Croner, Olivier Léon, François Chedevergne

55th 3AF International Conference on Applied Aerodynamics
23 – 25 March 2020, Poitiers - France

FP10-2020-croner

Industrial use of equivalent sand grain height models for roughness modelling in turbomachinery

Emma Croner [(1)], Olivier Léon[(2)] and François Chedevergne [(3)]
[(1)] *Safran Tech, Modelling & Simulation, Rue des Jeunes Bois, Châteaufort, 78114 Magny-Les-Hameaux, France, Email: emma.croner@safrangroup.com*
[(2)] *ONERA/DMPE, Université de Toulouse, 2 avenue Edouard Belin, 31055 Toulouse, France, Email: olivier.leon@onera.fr*
[(3)] *ONER/DMPE, Université de Toulouse, 2 avenue Edouard Belin, 31055 Toulouse, France, Email: francois.chedevergne@onera.fr*

ABSTRACT

The equivalent sand grain height principle is often used for modelling the effect of wall roughness in Reynolds-Averaged Navier-Stokes (RANS) simulations on industrial applications because it implies no additional cost compared to smooth-wall simulations and it is easy-to-use. This study aims at assessing the validity of such models for rough surfaces that are representative of industrial processes. Velocity profiles extracted from RANS simulations are validated against Particle Image Velocimetry (PIV) measurements on a flat plate configuration. It is shown that RANS models based on the principle of equivalent sand grain height are valid for real products' roughness. However, the arithmetic averaged height R_a does not appear to be linearly linked to the equivalent sand grain height h_s. Additional numerical applications on compressor test case highlight the important impact of such a hypothesis on the estimation of the performances of turbomachinery components.

1. INTRODUCTION

Mastering the surface roughness of turbomachinery blades is of first importance for both aerodynamic performances and manufacturing costs [1] [2]. This issue of surface roughness has been addressed for decades through experimental and numerical works. Based on Nikuradse's pipe flow experiments performed in the 1930's [3] [4], many authors analysed surface roughness effects relying on the concept of equivalent sand grain height, i.e. the sand grain height that leads to the same friction coefficient in the fully rough regime in Nikuradse's experiments. Several numerical models for Reynolds-Averaged Navier-Stokes (RANS) simulations also rely on this equivalence associated with the hypothesis of outer boundary layer similarity proposed by Townsend [5] [6]. Nonetheless, no universal correlation has been found to link real 3D roughness morphology to its sand grain equivalent. Bons [1] gives a review of correlations estimating the equivalent sand grain height mainly from the arithmetic averaged height R_a or quadratic averaged height R_q. Goodhand *et al.* [7] highlight the intrinsic limitations of using the R_a parameter. Recent experimental and numerical works show the validity of Townsend's similarity on 3D surfaces and suggest to add density or shape parameters in the calculation of the equivalent sand grain height [8] [9] [10].

This study aims at assessing equivalent sand grain height modelling for 3D rough surface extracted from real turbomachinery blades. The limitation of using R_a as the only characteristic parameter is also discussed. For this purpose, flat-plates experiments were performed on two roughness patterns extracted from measurements on real blades, obtained by two different manufacturing processes. Particle Image Velocimetry (PIV) measurements were used to analyse velocity profiles in the turbulent boundary layer and to extract equivalent sand grain heights. Comparisons with RANS simulations of the experimental configuration were used to investigate the validity of equivalent sand grain height concept and models. Applications on compressor test cases are also shown to highlight the impact of errors in the estimation of equivalent sand grain height in an industrial context.

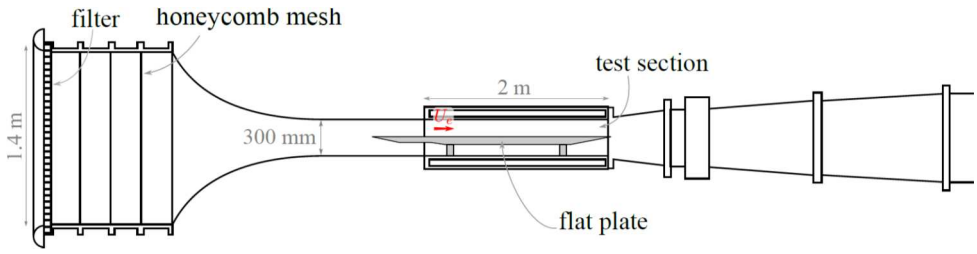

Figure 1. Schematic of the wind tunnel facility

2. EXPERIMENTAL SET-UP

The experimental test campaign was conducted in an Eiffel-type low-speed wind tunnel at ONERA Toulouse, illustrated in Fig. 1.

Several rough samples of 1000 mm x 200 mm were mounted and adjusted on a flat plate placed in the wind tunnel test section with no angle of attack. Each sample was composed of five consecutive plates of 200 mm x 200 mm as shown in Fig. 2. The boundary layer developing on the flat plate was triggered upstream of the sample near the leading edge of the plate.

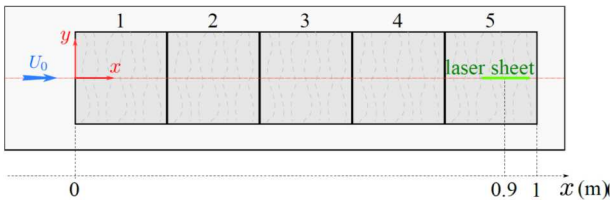

Figure 2. Positions of the rough samples and the PIV laser sheet on the experimental flat plate.

The samples selected in this project are representative of several real products' roughness. The topologies of these selected surfaces were measured by 3D optical scanners that provided plan elevation maps, i.e. CAD models of the rough surface without the shape of the piece. These CAD's were then scaled according to the boundary layer thickness in the test section that is approximately 30 mm at the axial measurement position. This scaling aimed at providing maximum peak-to-peak roughness heights of 3 to 4 mm.

In the present study we only consider two samples identified as samples A and B. Photographs of these two samples at similar scales are shown in Fig. 3. After scaling, they both exhibited similar R_a values (~0.55 mm) but very different statistics and characteristic length scales in their patterns. These samples were 3D-printed by Manutech USD using a SLM method that was considered as satisfactory for the present purpose since the surface roughness induced by the printing powder was more than one order of magnitude smaller than the roughness length scales studied.

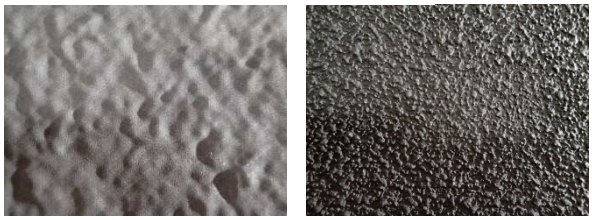

a) Sample A - R_a= 0.56 mm b) Sample B - R_a=0.53 mm

Figure 3. Photography of the two rough samples.

Two-dimension (2D) two-component (2C) Particle-Image Velocimetry (PIV) was used for the characterisation of velocity profiles in the turbulent boundary layers developing over the rough surfaces. The measurement plane was located 900 mm downstream of the onset of the rough sample to ensure measurements in the fully developed region.

The measurement methodology was assessed on a smooth-wall case by comparing the mean and root-mean-square profiles of the axial velocity to theoretical and semi-empirical laws proposed in the literature, providing confidence in the results.

The friction coefficients induced by the two wall roughness samples were estimated using an indirect method: the friction velocity U_τ was estimated from near-wall cross components of the Reynolds stress tensor relying on Eq. 1:

$$U_\tau{}^2 \approx -\overline{u'v'}_{wall} \qquad (1)$$

This method was successfully used by Ligrani *et al.* [11] for example. The equivalent sand grain height was then estimated from the friction velocity by the use of Grigson-Colebrook law [12].

3. NUMERICAL SET-UP

Steady bi-dimensional (2D) Reynolds-Averaged Navier-Stokes (RANS) simulations were run with elsA CFD software [13], based on a cell-centred finite volume discretization.

The numerical domain used in RANS simulations aims at reproducing the experimental set-up by simulating the central plane of the test section.
Inflow conditions were specified from stagnation quantities, i.e. total pressure and enthalpy, calculated from experimental data. A low turbulent intensity of 0.4% was imposed to mimic the natural turbulence rate of the facility. Constant static pressure at the outlet was imposed to match the channel velocity at the measurement plane out of the boundary layer. A no-slip condition was finally imposed at the walls and a roughness condition, prescribed by its equivalent sand grain height h_s, was used on the sections containing the rough samples.

The block-structured computational mesh was created with ICEM CFD meshing software. It consists of 192.000 hexahedral cells. A first cell size of 1 micron at walls enabled a fine resolution of the boundary layers according to wall unit values (y^+<0.1). A ratio of 1.05 was used in longitudinal and normal directions.

The simulations were fully turbulent. Turbulence closure was ensured by Menter's two-equation k-ω model in its baseline (BSL) version [14]. Roughness modelling was based on the equivalent sand grain height approach, i.e. the turbulent boundary conditions at the wall were modified to simulate the effect of roughness on the friction factor and to induce an off-set on the boundary layer logarithmic law. The formulation was the one proposed by Aupoix [15] based on Grigson-Colebrook correlation between normalized velocity off-set and normalized equivalent sand grain height [12].
The spatial discretisation used the second-order accurate scheme of Roe with a limiter of 0.01 in Harten correction for both conservative and turbulent fields. A maximal Courant-Friedrich-Levy (CFL) number of 20 was used for pseudo-time resolution. For all testing conditions, simulations consisted in a 100.000-iteration run which ensured convergence of the residuals, the channel mass flow rate, the drag on the rough samples and the boundary layer characteristics at the measurement plane.

The idea of the study is to analyse the precision of the whole methodology and not to compare roughness effect at fixed boundary layers condition. It is assumed that numerical schemes, turbulence modelling and transition from smooth to rough boundaries will introduce errors.

4. RESULTS

4.1 Equivalent sand grain heights

Tab. 1 summarizes the R_a measurements and the experimental estimations of the equivalent sand grain heights h_s for the two considered samples. It also contains the heights estimated from the correlation proposed by Koch & Smith [15]:

$$h_s = 6.2R_a \quad (2)$$

	Sample A	Sample B
R_a	0.56	0.53
h_s - Exp.	0.15	2.85
h_s - [15]	3.46	3.28

Table 1. Roughness characteristics of the samples.

The normalized velocity profiles obtained with RANS simulations using the experimental values of h_s are presented in Fig. 4 and compared with both experimental results and a smooth reference. These results show that RANS modelling based on equivalent sand grain heights enabled reproducing the effect of 3D realistic roughness. The external part of the velocity profile is shifted downwards by the friction increase. Using experimental values of h_s provided very good results for sample A. The results were less precise for sample B.

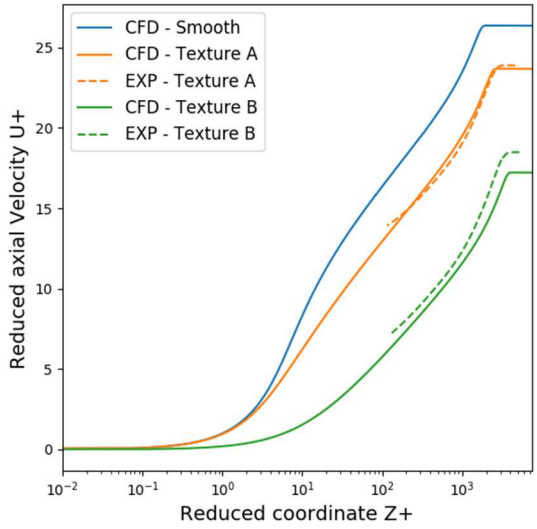

Figure 4. Comparison of normalised axial velocity profiles between experiments and RANS simulations.

Another major results illustrated by Tab. 1 and Fig. 4 is the important difference between the effects of the two samples despite similar R_a values. A ratio of 19 is obtained between the two experimental values of h_s inducing a significant change in velocity profile. This observation confirm several previous works [7] [8] indicating that averaged roughness heights cannot be sufficient to characterize the effect of a wall texture.
To complete this observation, Fig. 5 and Fig. 6 compare results obtained using the experimental h_s with those obtained using the correlation of Koch & Smith as CFD simulation input. They show that the correlation seems good for sample B but is not adapted for sample A. The comparison with a smooth reference even show that

using this correlation for texture A leads to worse results than a smooth simulation.

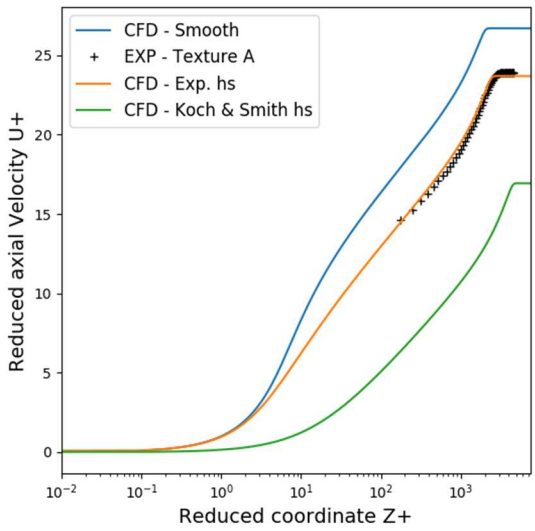

Figure 5. Comparison of normalised axial velocity profiles obtained from experimental h_s and Koch & Smith [16] correlation with experimental results for sample A.

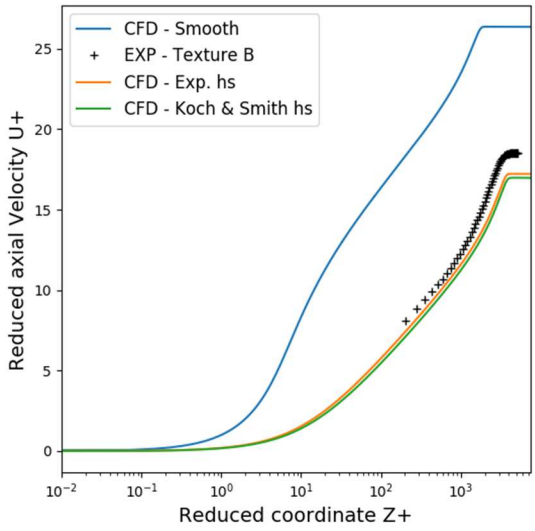

Figure 6. Comparison of normalised axial velocity profiles obtained from experimental h_s and Koch & Smith [16] correlation with experimental results for sample B.

4.2 Boundary layer regimes

The validity of the previous RANS modelling and aerodynamic analysis of the experimental velocity profiles is highly dependent on the state of the boundary layer developing over the rough surfaces. Several points thus needed to be investigated to better interpret the results obtained in Section 4.1: the turbulent state of the boundary layers, their fully-developed state and the roughness regime achieved.

The first two points are easily verified and the main discussion here focused on the flow regime that can be hydraulically smooth, transitionally rough to fully rough. The modification of the normalised velocity profile compared to a smooth-wall case indicates a rough regime but not that the fully rough regime is reached, i.e. that the friction coefficient does not depend on the Reynolds number anymore.
To investigate this point, the "diagnostic plot" of the boundary layer is plotted in Fig. 7 and Fig. 8 for samples A and B respectively. These plots compare the experimental boundary layer with the canonical case reported by Alfredsson *et al.* [17] for a fully turbulent boundary layer on a smooth wall in a zero pressure gradient configuration and with the linear regression by Castro *et al.* [18] for the fully rough regime.

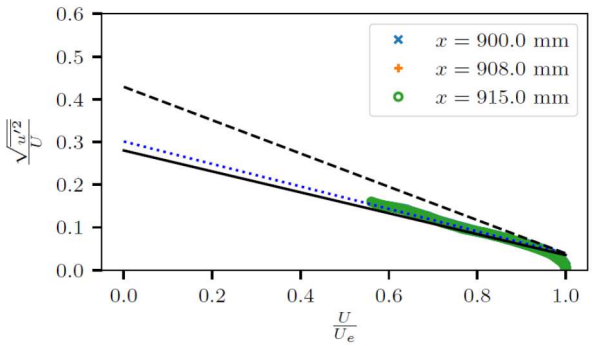

Figure 7. Diagnostic of experimental velocity profiles measured on sample A. Comparison with smooth fully turbulent case by Alfredsson *et al.* [17] (plain line) and fully rough regime by Castro *et al.* [18] (dotted line)

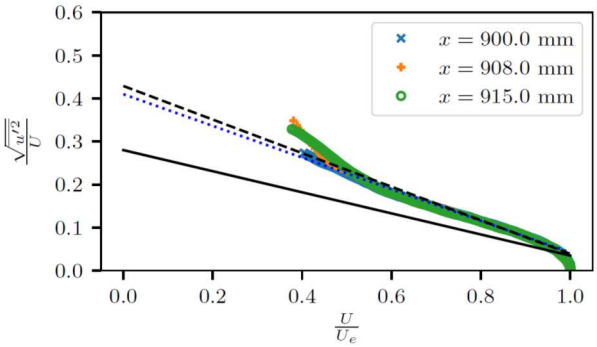

Figure 8. Diagnostic of experimental velocity profiles measured on sample B. Comparison with smooth fully turbulent case by Alfredsson *et al.* [17] (plain line) and fully rough regime by Castro *et al.* [18] (dotted line)

These diagnostic plots show that the fully rough regime is reached only on sample B, which exhibits the highest h_s. The boundary layer remains in a transitionally rough regime for sample A.
For this reason, several flow velocities were tested in the experimental testing campaign for sample A. Velocity was increased from 21 m/s to 58 m/s without reaching fully rough regime yet. For the experimental results of sample A, note that the value indicated in Tab. 1 is the one obtained for the maximal velocity of 58 m/s.
These results confirm that R_a is not sufficient for roughness characterization and consequently for the design of rough samples in experimental campaigns. Looking at photography of Fig. 3, it is important to note that sample A is the one exhibiting the longest spatial wave lengths in its roughness content, i.e. the longest characteristic length scales along the plate. It can hence be linked to surface referred as "wavy" in previous works reported in the literature [8] [19]. Interestingly, Nugroho *et al.* [19] found that fully rough regime cannot be reached in their experiments for this kind of surfaces.

The various velocities that were tested on sample A enable to study the reproduction of the Reynolds number effect in a transitionally rough regime by the numerical modelling. Fig. 9 show the comparison of experimental profiles obtained from PIV and numerical profiles for $h_s = 0.15$ mm at various external velocities. Fig. 10 is a zoom of Fig. 9 in the logarithmic and external zones of the normalised velocity profiles.

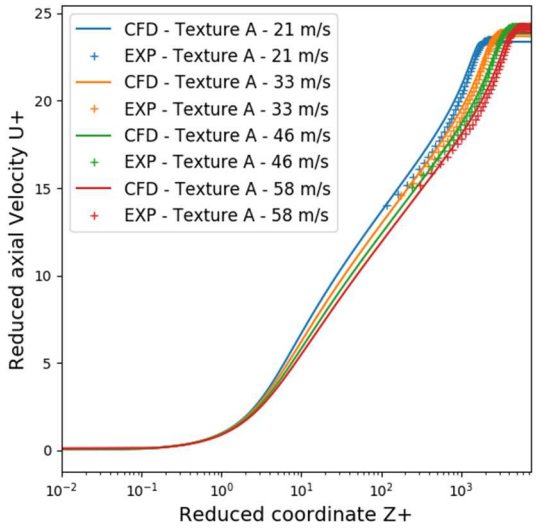

Figure 9. Comparison of normalised axial velocity profiles between experiments and RANS simulations for various flow velocity on sample A

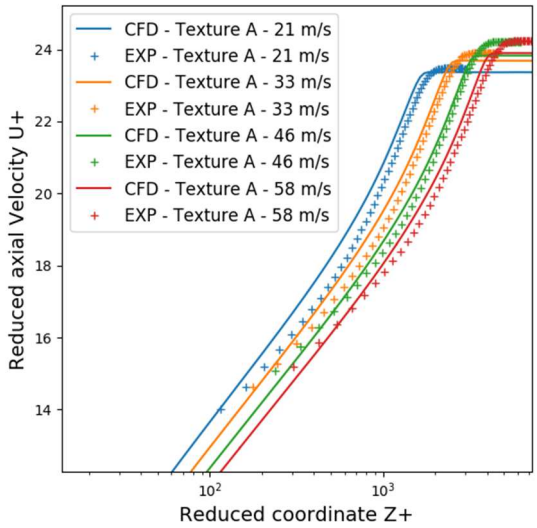

Figure 10. Comparison of normalised axial velocity profiles between experiments and RANS simulations for various flow velocity on sample A – Zoom on the logarithmic and external zones

The results show an effect of the channel velocity on the external normalised velocity U_e^+ and consequently on the friction coefficient. This confirms the transitionally rough regime but this also shows that the effect is quite well reproduced by simulations based on the concept of equivalent sand grain height. Getting experimental results in the transitionally rough regime does only impact the precision of equivalent sand grain height estimation if too far from fully rough regime. Indeed, by definition, surfaces with the same equivalent sand grain height exhibit same friction coefficient in the fully rough regime. In this case, h_s values vary between 0.15 mm and 0.21 mm depending on the channel velocity.

4.3 Application on compressor test cases

Flat plate experiments and simulations highlight that the equivalent sand grain height concept is able to reproduce the effects of roughness on the wall friction and the velocity profiles but that using R_a as the only characteristic parameter of a surface roughness may lead to significant errors. In order to quantify the impact of such an error on industrial applications, rough simulations were ran on compressor test cases.
It is assumed here that standard R_a of a blade is 1 micron. By consideration of h_s/R_a ratios estimated from Tab. 1, we can infer representative values of h_s between 0.25 microns (equivalent to sample A) and 10 microns (equivalent to sample B).

Two test cases were considered for this demonstration. The first one is the Rotor 37 from NASA [20] [21], a single-rotor case illustrated in Fig. 11. The second one is the 3.5-stage high-speed compressor CREATE [22] illustrated in Fig. 12.

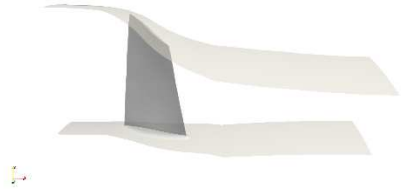

Figure 11. Geometry of the Rotor 37 test case – Visualisation of walls in the computational domain

Figure 12. Geometry of the CREATE test case – Visualisation of walls in the computational domain

For these two cases, RANS simulations were computed with roughness modelling on all walls, including blades, hubs and shrouds. The numerical parameters are similar to those described in section 3, including the use of k-ω BSL turbulence model. All simulations use a steady resolution and periodicities are imposed to simulate only one blade for each row. The rotor-stator interfaces of the multi-stage case is treated with boundary conditions of mixing plane type (azimuthal averages).
Tab. 2 summarises the pressure ratio and isentropic efficiency obtained.

	Rotor 37	CREATE
Pressure ratio	-0.0103	-0.0575
Isentropic efficiency	-0.0155	-0.0110

Table 2. Differences in global performances of compressor test cases between h_s of 0.25 and 10 microns

RANS simulations of the two test cases indicate that an equivalent sand grain height of 0.25 microns leads to the same results than a smooth correlation. The boundary layers are still in the smooth regime. For an equivalent sand grain height of 10 microns, the rough regime is reached and the consequences on the global performances are significant with a loss of more than 1 point of isentropic efficiency for these two compressor cases.
This confirm that the estimation of the input of the simulations, i.e. the equivalent sand grain heights is of first importance for industrial applications and that linear relations with R_a are not relevant.

5. CONCLUSION

Results highlight both the validity of the theory of this modelling and the limitation of using R_a parameter for the determination of equivalent sand grain heights. This equivalent sand grain height appears to be 20 times higher on the second texture despite similar arithmetic averaged heights R_a. In this context, using correlations based uniquely on R_a, like the one proposed by Koch & Smith, may lead to results even less precise than smooth-wall simulations. Additional RANS simulations were run on compressor test cases to show the impact of such a difference in estimated equivalent sand grain heights for industrial applications.
As a result, equivalent sand grain height concept can be used for modelling realistic rough surface but the key point for the precision of simulations is the estimation of this characteristic height.
Further investigations are also required to estimate the precision of this modelling on turbomachinery configurations. The model is based on the study of fully developed, fully turbulent boundary layers, which are not representative of blades boundary layers. The effect of such hypothesis on the estimation of the performances of rough turbomachinery components has to be evaluated.

6. ACKNOWLEDGEMENT

This study has been founded by Safran Group. The authors acknowledge Manutech USD for the manufacturing of the 3D-printed rough samples.

7. REFERENCES

1. Bons, J. P. (2010). A review of surface roughness effects in gas turbines, *Journal of Turbomachinery,* 132(2):021004

2. Goodhand, M. N. (2015). Admissible roughness in gas turbines, *Proceedings of the ASME Turbo Expo 2015: Turbine Technical Conference and Exposition*, Montréal, Canada, 2015

3. Nikuradse, J. (1933). Strömungsgesetze in rauhen Rohren, VDI-Forschungsheft 361.

4. Nikuradse, J. (1950). Laws of flows in rough pipes, NACA Technical Memorandum 1292.

5. Townsend, A. A. (1980). *The Structure of Turbulent Shear Flow*, Cambridge University Press.

6. Raupach, M.R., Antonia, R. A. & Rajagopalan, S. (1991). Rough-wall turbulent boundary layers, *Applied Mechanics Reviews*, 44(1), pp. 1-25.

7. Goodhand, M. N., Walton, K., Blunt, L., Lung, H. W., Miller, R. J. & Marsden, R. (2015). The limitations of using "Ra" to describe surface roughness, *Proceeding of ASME Turbo Expo 2015: Turbine Technical Conference and Exposition*, GT2015-43326.

8. Flack, K. A. & Schultz, M. P. (2014). Roughness effects on wall-bounded turbulent flows, *Physics of Fluids*, 26:101305.

9. Thakkar, M., Busse, A. & Sandham, N. (2016). Surface correlations of hydrodynamic drag for transitionally rough engineering surfaces, *Journal of turbulence*, 18(2), pp. 138-169.

10. Forooghi, P., Stroh, A., Magagnato, F., Jakirlic, S. & Frohnapfel, B. (2017). Toward a Universal Roughness, *Journal of Fluids Engineering*, 139(12):121201.

11. Ligrani, P. M. & Moffat, R. J. (1986). Structure of transitionally rough and fully rough turbulent boundary layers, *Journal of Fluid Mechanics*, 162(11), pp. 69-98.

12. Grigson, C. (1992). Drag losses of new ships caused by hull finish, *Journal of ship research*, 36, pp. 182-196.

13. Cambier, L, Gazaix, M., Heib, S., Plot, S., Poinot, M., Veuillot, J., Boussuge J.-F. & Montagnac, M. (2011). An overview of the multi-purpose elsA flow solver, *Journal Aerospace Lab*, 2, pp. 1-15.

14. Menter, F. R. (1994). Two-equation eddy-viscosity turbulence models for engineering applications, *AIAA Journal*, 32(18), pp. 1598-1605.

15. Aupoix, B. (2007). A general strategy to extend turbulence models to rough surfaces : Application to Smith's k-l model, *Journal of Fluids Engineering*, 129, pp. 1245-1254.

16. Koch, C. & Smith, L. (1976). Loss sources and magnitudes in axial-flow compressors, *Journal of Engineering for Power*, pp. 411-424.

17. Alfredsson, P. H., Segalini, A. & Örlü, R. (2011). A new scaling for the streamwise turbulence intensity in wall-bounded turbulent flows and what it tells us about the "outer" peak, *Physics of Fluids*, 23(14).

18. Castro, I. P., Segalini, A. & Alfredsson, P.H. (2013). Outer-layer turbulence intensities in smooth- and rough-wall boundary layers, *Journal of Fluid Mechanics*, 727, pp. 119-131.

19. Nugroho, B., Utama, I. K. A. P., Monty, J.P., Hutchins, N. & Ganapathisubramani, B. (2018). The influence of in-plane roughness wavelength relative to the turbulent boundary layer, *ETMM11 ERCOFTAC Symposium*, Palermo.

20. Reed, L. & Moore, R. D. (1978). Design and overall performance of four highly loaded, high speed inlet stages for an advanced high-pressure-ratio core compressor, *NASA Technical Paper 1337*, Cleveland, USA.

21. Dunham, J. (1998). CFD Validation for Propulsion System Components, *AGARD Advisory Report 355*, Neuilly-sur-Seine, France.

22. Ottavy, X., Courtiade, N. & Gourdain, N. (2012). Experimental and Computational Methods for Flow Investigation in High-Speed multistage Compressor, *Journal of Propulsion and Power*, 28(16), pp. 1141-1155.